Laser Ionization Measurements of the Photodissociation Kinetics of Jet-Cooled Benzaldehyde

Cristina R. Silva[†] and James P. Reilly*

Department of Chemistry, Indiana University, Bloomington, Indiana 47405

Received: February 27, 1997; In Final Form: August 4, 1997[⊗]

The kinetics of benzaldehyde dissociation into benzene and carbon monoxide following excitation to the S_2 state has been investigated under jet-cooled conditions by two-color laser ionization mass spectrometry using a pump−probe technique. A kinetic model has been proposed to explain the observed biexponential decay of the benzaldehyde signal and the single-exponential growth of the benzene product signal in terms of a sequential decay of two excited states of benzaldehyde, one of which leads to formation of benzene molecules in its lowest triplet state. Reactant disappearance and product appearance rates were determined for a number of vibronic transitions in the first 2000 cm^{-1} energy region of the S_2 state. At the S_2 origin the decay rate of the short-lived state of benzaldehyde was found to be 1.2×10^6 s^{-1}.

Introduction

Benzaldehyde, the simplest aromatic carbonyl compound, is an interesting molecular system due to the presence of close-lying $\pi\pi^*$ and $n\pi^*$ states. Intersystem crossing (ISC) is favored by spin−orbit coupling, and excitation to the singlet states is followed by phosphorescence, not by fluorescence. A reactive channel leading to dissociation into benzene and carbon monoxide is observed following activation to $S_2(\pi\pi^*)$. We have recently reported the excitation spectrum of jet-cooled benzaldehyde in the $S_2 \leftarrow S_0$ absorption band.[1] In the present work we employ the same experimental apparatus to investigate the kinetics of dissociation of jet-cooled benzaldehyde following excitation of different vibronic levels in the S_2 state and to explore the relaxation dynamics of its excited states under isolated conditions.

The photodissociation of benzaldehyde has been investigated by photolysis,[2,3] phosphorescence emission,[2−8] and multiphoton ionization mass spectrometry[9−17] experiments. Berger et al.[2] reported that following irradiation into the S_2 band of benzaldehyde vapor at 276 nm, benzene and carbon monoxide were detected by gas chromatography. The dissociation quantum yield was found to be pressure dependent, tending toward unity at very low pressures. Bruhlmann et al.[3] observed that photolysis of a mixture of equal parts of benzaldehyde-h_6 and benzaldehyde-d_6 at 276 nm produced exclusively benzene-h_6 and benzene-d_6, and they proposed a concerted reaction mechanism. Excitation to $S_1(n\pi^*)$ with wavelengths of 328 and 365 nm, on the other hand, did not lead to benzene or carbon monoxide formation.[2]

A number of groups have investigated the wavelength and pressure dependence of the phosphorescence emission of benzaldehyde.[2−8] As reported by Baba and co-workers,[5,6] the relative phosphorescence quantum yield is nearly constant throughout the S_1 and S_2 regions at higher pressures (600 mTorr), while at low pressures (2 mTorr) it decreases abruptly at the onset of the S_2 absorption band. These results were interpreted in terms of an increase in the efficiency of a nonradiative relaxation pathway in S_2 leading to dissociation. At low pressures, collisional deactivation is slow and dissociation occurs with consequent suppression of emission. At higher pressures, collisional deactivation is faster than dissociation, and the result is that the emitting state is populated. The shape of the wavelength-resolved phosphorescence spectrum was found to be independent of pressure with the emission originating from the vibrationless level of $T(n\pi^*)$.[2,6] The vapor-phase emission of benzaldehyde has been observed under high resolution in a number of studies.[18−24] Apart from some weak E-type delayed fluorescence,[6,22] emission occurs from the vibrationless level of $T(n\pi^*)$, with the CO stretching vibration being the dominant accepting mode. These results are in agreement with molecular orbital calculations[1] that predict that the largest geometric change on $n\pi^*$ excitation corresponds to a substantial lengthening of the CO bond.

Laser-induced multiphoton ionization mass spectrometry (MPI/MS) has also been used to investigate the photodissociation of benzaldehyde.[9−17] The general trend observed is that extensive benzene ion formation occurs following excitation into $S_2(\pi\pi^*)$, while mainly benzaldehyde ions are observed following excitation to $S_1(n\pi^{**})$. The presence of benzene ions in the MPI mass spectrum of benzaldehyde can be explained either by ionization of neutral benzene formed as a product in the photodissociation of benzaldehyde or by fragmentation of benzaldehyde ions. El-Sayed and co-workers[14,15] studied the ionization−fragmentation mass pattern of benzaldehyde using nanosecond laser pulses at 355 and 266 nm and concluded that both processes occurred, the predominance of either one being a function of excitation wavelength and laser intensity.[14] Using 266 nm picosecond laser pulses, only C_6H_5CO radical cations were detected, indicating that further photon absorption occurred before dissociation of benzaldehyde into neutral benzene took place following the excitation step.[15] Since large amounts of benzene ions were observed using nanosecond duration laser pulses, they concluded that the dissociation lifetime of benzaldehyde following excitation to S_2 at this wavelength should lie in the picosecond to nanosecond time range.

Photoelectron spectroscopy has been used to identify the benzene ion precursor as neutral ground-state benzene. Reilly and co-workers[13] reported that, when benzaldehyde is irradiated at 258.9 nm, the observed laser photoelectron spectrum is identical with that of benzene at this wavelength. This has been interpreted as resonant stepwise ionization of benzene molecules formed in the ground state following dissociation of benzaldehyde.

Polevoy et al.[16,17] employed two-color laser ionization pump−

[†] Permanent address: Instituto de Química, Departamento de Físico-Química, Universidade Federal do Rio de Janeiro, Cidade Universitária CT Bloco A, Rio de Janeiro, RJ, 21949-900, Brazil.

[⊗] Abstract published in *Advance ACS Abstracts,* September 15, 1997.

S1089-5639(97)00755-X CCC: $14.00

probe experiments to investigate the dissociation time scale of benzaldehyde over a range of excitation wavelengths in the S_2 absorption band. They observed the kinetics of disappearance of the reactant and appearance of the benzene product by following the production of ions of these species as a function of the time delay between the excitation and the ionization steps. The rate of formation of benzene ions was found to be related to the rate of disappearance of benzaldehyde ions, which, in turn, was observed to increase exponentially with excitation energy.

All of the above studies involved room-temperature gas-phase molecules. The absorption and excitation spectra of benzaldehyde in the $S_2 \leftarrow S_0$ region[2,4,25−27] are structured but highly congested under these conditions. Apart from our recent excitation spectrum,[1] no other studies have probed the S_2 state under jet-cooled conditions. The nπ^* states, in contrast, have received more attention. In the past decade a number of studies have addressed the spectroscopy and dynamics of these states under free-jet conditions.[28−31] In the present work we use a supersonic expansion to obtain rotationally and vibrationally cold benzaldehyde molecules that allow us to prepare a well-defined single vibronic level of the excited state. Furthermore, the molecules travel under collision-free conditions, and the dissociation kinetics can be observed without the interference of collisional processes. A pump−probe technique similar to that employed by Polevoy et al. is used. The pump laser excites the molecule to a resonant (single vibronic) level of the S_2 state, and the probe laser, delayed by a variable time, interrogates the population of the transient states.

Experimental Section

The experimental apparatus employed to record two-color photoionization mass spectra has been recently described.[1] Briefly, the frequency-doubled output of a XeCl excimer-pumped dye laser provided 80 μJ/pulse of exciting (pump) radiation with a bandwidth of less than 0.4 cm^{-1}, a pulse duration of 3−5 ns, and a cross section of about 3 × 5 mm at the ionization region. A VUV F_2 laser connected to the mass spectrometer through an evacuated glass tube provided 6 ns pulses of 157 nm ionizing radiation. This was collimated by a set of four apertures to produce a beam having a cross section of about 4 × 6 mm, as measured by the light emitted in the visible red. The apertures could be moved along the beam path in order to maximize ion signal. Due to its VUV nature, the probe laser pulse energy was not actually measured, but from the fraction of the beam cross section that reached the ionization region, it was estimated to be less than 0.3 mJ. The two laser beams counterpropagated coaxially intercepting the molecular beam orthogonally in the interaction region of our time-of-flight mass spectrometer 15 cm downstream from the supersonic nozzle.

The supersonic molecular beam consisted of a mixture of approximately 1 Torr of benzaldehyde vapor seeded in 1.5 atm of argon. The gas mixture was expanded through a 0.75 mm diameter pulsed nozzle into the mass spectrometer chamber where an average pressure of 2 × 10^{-5} Torr was maintained. Under these expansion conditions the molecular beam traveled at a speed of 600 m/s as determined by measurements of the shift in the time of arrival of benzaldehyde molecules at the interaction region caused by changes in the nozzle to interaction region distance. On the basis of this measurement and on the shapes of the two overlapping beams, we estimate that molecules pass through the light interaction region in about 4 μs. Any process that occurs on a time scale much longer than this cannot be studied with this apparatus.

A pulse generator was used to fire the pulsed valve and trigger a delay generator that provided the delay time for cold benzaldehyde molecules to reach the ionization region. The delay generator simultaneously triggered the pump laser and a boxcar averager (EG&G Princeton Applied Research Model 162). The latter was used as a variable delay generator to trigger the probe laser. Time intervals of 2.17 ± 0.02 and 5.35 ± 0.02 μs were scanned at an approximate resolution of 10 ns/point, each point corresponding to 20 laser shots. Due to the relatively short operating life of the F_2 laser gas mixture, the laser pulse energy dropped by 10−20% during the 4−9 min required to scan these delay ranges at a repetition rate of 20 Hz. This decay could not be neglected, and a procedure to correct the ion signal for laser energy fluctuations is described below.

The ion signal was detected by a microchannel plate detector, recorded by a waveform digitizer (Biomation 6500) and accumulated in a microcomputer. The digitizer was always triggered by the probe laser so ions formed by two-color ionization have the same flight time independent of the delay between the lasers. Ions of the carrier gas produced by photoemission electron impact ionization[32] induced by the VUV radiation ($h\nu_{\text{ioniz}} = 7.9$ eV) hitting the interior walls of the mass spectrometer[1] were used to monitor the F_2 laser energy. The Ar^+ ion current was assumed to be proportional to the energy of the probe laser, and it was used as a normalizing factor to correct the benzaldehyde and benzene ion signals for variations in the pulse energy of the probe laser. The pump laser pulse energy remained constant, as indicated by measurements performed before and after each scan.

To verify the precision of the normalization procedure, the pump−probe delay was scanned forward and backward. In the forward scan, as already described, the pump laser was fired at a fixed time after the pulsed valse and the probe laser was delayed relative to the pump pulse. In the backward scan, the pump−probe delay was decreased by delaying the pump laser trigger signal while the probe laser was fired at a fixed time relative to the pulsed valve. These two arrangements excited and probed slightly different parts of the molecular beam. However, since the molecular beam pulse displayed a fwhm of more than 100 μs, the molecular density did not vary significantly over a 5 μs time interval (see Figure 8, ref 1, for molecular beam shape). Decay rates obtained with the two arrangements were the same within 10−20%.

Results

Mass Spectra. In an initial experiment to investigate the S_2 state dynamics of benzaldehyde we employed an ArF laser as the source of the probe radiation. Extensive benzene ion formation was observed when benzaldehyde was irradiated with this 193 nm light alone. Since the absorption maximum of the $S_4 \leftarrow S_0$ band, the strongest band in the optical spectrum of benzaldehyde, lies around 194−195 nm,[33,34] this was interpreted as the result of fast dissociation of S_4 benzaldehyde molecules followed by ionization of the nascent benzene molecules. The F_2 laser radiation, on the other hand, provided an efficient way of ionizing electronically excited benzaldehyde without exciting ground-state benzaldehyde molecules. We have successfully used this radiation to record the two-color ionization excitation spectrum of jet-cooled benzaldehyde in this region.[1]

Under the light conditions employed, benzaldehyde ions were observed only with two-color ionization. but ions of the carrier gas (Ar^+ and Ar^{2+}) were produced whenever the F_2 laser was employed (see Figure 6, ref 1, for a comparison of one- and two-color ionization mass spectra). The mechanism responsible for the formation of the latter ions, electron impact ionization,

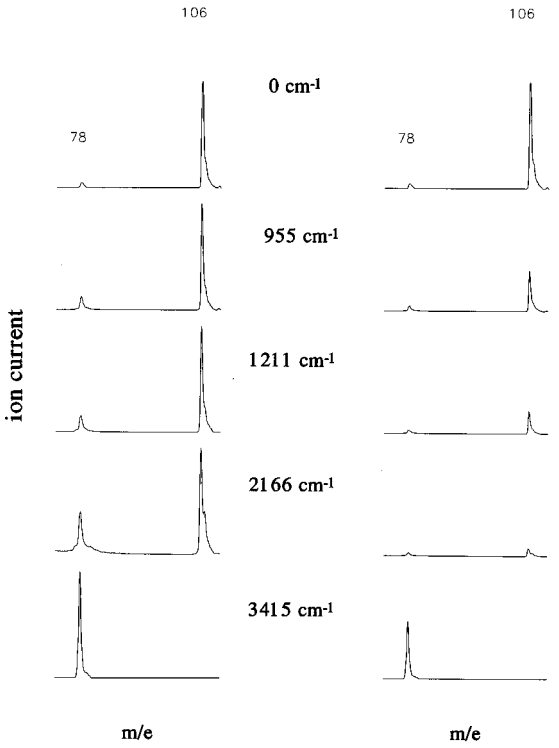

Figure 1. Two-color photoionization mass spectra of jet-cooled benzaldehyde as a function of excess energy above the S_2 origin. Peaks at $m/e = 78$ and 106 are assigned to benzene and benzaldehyde ions, respectively. Left column: spectra scaled so that the tallest peak is the same height. Right column: spectra normalized to light intensity (peaks are proportional to absolute ion yields).

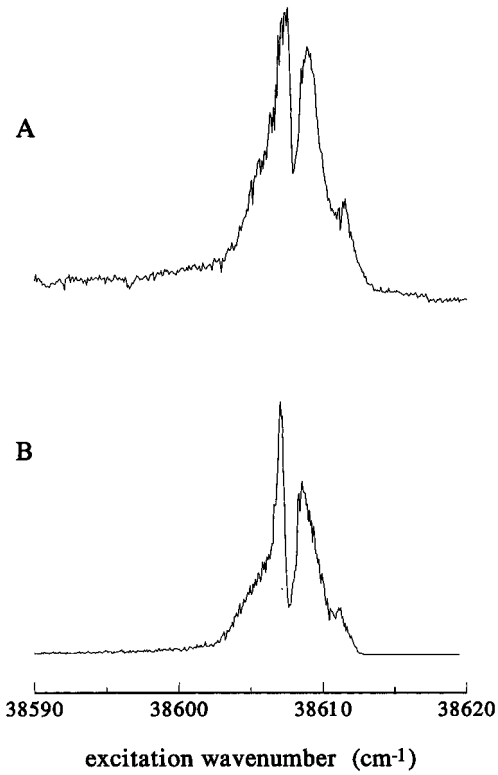

Figure 2. Photoionization excitation spectra of jet-cooled benzaldehyde (A) and benzene (B) in the region of the 6_0^1 $S_1 \leftarrow S_0$ transition of benzene: (A) two-color ion signal at $m/e = 78$; (B) one-color ion signal at $m/e = 78$.

did not lead to any other ions because all other species were present at much lower abundance than argon. As for the dissociation reaction products, CO ions were not detected with any combination of the two lasers, whereas benzene ions were produced not only by two-color ionization but, at excitation wavelengths corresponding to allowed transitions in the $S_1 \leftarrow S_0$ spectrum of benzene, by one-color ionization with the pump laser.

Figure 1 displays a series of two-color ionization mass spectra of jet-cooled benzaldehyde taken at different excitation energies within the S_2 band. The probe laser was fired 10−20 ns after the pump laser in order to allow some buildup of the benzene population. In the left-hand column, each spectrum has been scaled so that the tallest peak has the same height in order to compare the relative amounts of benzene and benzaldehyde ions produced at different excitation frequencies. The same data are displayed in the right-hand column but with peak heights being proportional to absolute ion yields. A trend clearly identified in this figure is that the $C_6H_6+/C_6H_5CHO^+$ ratio increases (left column) while the absolute benzaldehyde ion yield decreases (right column) with excess energy. These results are understood in terms of an increase in the dissociation rate with excitation energy, a point that is confirmed by the time-dependent measurements to be presented.

Note that the excitation frequency (3415 cm^{-1} above the 35 191 cm^{-1} S_2 origin) of the two-color ionization mass spectra shown at the bottom of Figure 1 corresponds to the frequency of the 6_0^1 $S_1 \leftarrow S_0$ transition of benzene.[35,36] At this excitation frequency, benzene ions can be observed with the pump laser alone. They are produced through a resonant process in which benzene molecules in the vibrationless ground electronic state are electronically excited and then ionized. The resonance enhancement that occurs at this particular excitation frequency is discussed in the next section.

Wavelength Dependence. The $S_2 \leftarrow S_0$ absorption band of benzaldehyde that extends from 284 nm to approximately 250 nm is featureless below 270 nm under room-temperature[2] and jet-cooled[1] conditions. While acquiring the two-color excitation spectrum of benzaldehyde,[1] we noted that at some wavelengths there was a significant enhancement of the benzene ion signal even though the benzaldehyde ion signal displayed no spectral dependence on the excitation step. This occurred at wavelengths corresponding to the 6_0^1 and 6_1^0 transitions of the $^1B_{2u} \leftarrow {}^1A_{1g}$ band of benzene. As mentioned above, enhancement of the benzene signal at these wavelengths did not depend on the presence of the probe radiation; it could be observed when benzaldehyde was irradiated with the pump laser alone.

The wavelength dependence of the benzene ion signal in the 259 nm region is shown in Figure 2. Part A of this figure shows the wavelength dependence of the ion current observed at mass channel 78 when jet-cooled benzaldehyde is irradiated in this wavelength region. The signal displayed in part B is that obtained at the same mass channel when jet-cooled benzene is irradiated. The two bands are extremely similar, with the former being slightly wider. On the basis of the two observed rotational contours, we estimate rotational temperatures of 10 and 5 K. Irradiation of jet-cooled benzaldehyde in the region of the 6_1^0 $S_1 \leftarrow S_0$ transition of benzene below 267 nm led to a similar benzene-like wavelength dependence for the mass 78 ion signal. These results clearly show that the observed signal comes from the 1+1 one-color ionization of ground-state benzene molecules with either 0 or 1 quantum of vibrational excitation in mode 6. What is not absolutely clear is whether these molecules were already present in the benzaldehyde sample as an impurity or if they were formed in the photodissociation of benzaldehyde. Although we did not purify the benzaldehyde sample prior to its use, the latter hypothesis is consistent with previous mass spectrometry and photoelectron spectroscopy results obtained by this group.[13] Long et al. observed that, when benzaldehyde

is irradiated at 258.9 nm, the strongest peak in the mass spectrum, by 2 orders of magnitude, is at mass 78. In that experiment care was taken to remove any benzene present in the benzaldehyde sample by using a gas chromatographic inlet with the mass spectrometer. Since the benzaldehyde mass spectrum was unaffected by this separation and, in addition to that, the photoelectron spectrum of benzaldehyde at 258.9 nm was identical with that of benzene at this wavelength, the mass 78 peak was attributed to ground-state benzene molecules formed in the photodissociation of benzaldehyde. This assignment, however, leaves an excess energy larger than 4 eV to be distributed among translational motion of the reaction products and the vibrational and rotational degrees of freedom of CO. Such a product energy distribution seems unlikely under isolated molecule conditions.

An estimate of the relative population of benzene molecules in $v = 1$ and $v = 0$ following excitation of benzaldehyde has been made on the basis of our present measurements of the intensity ratio of the 6_1^0 to the 6_0^1 bands. The value thus obtained, 0.06 ± 0.02, is close to that reported by Atkinson and Parmenter[35] (0.056) for benzene under room-temperature conditions, but it is somewhat larger than that reported by Rice and co-workers[36] (0.023) for a jet-cooled benzene expansion. While, on one hand, the 6_1^0 to 6_0^1 band intensity ratio that we measured is roughly the same as that for a room temperature benzene sample, the contours of the 6_1^0 and 6_0^1 bands correspond to a sample with a rotational temperature about twice that of jet-cooled benzene. These limited results thus prevent us from drawing firm conclusions as to the relative amounts of benzene impurity and photoproduct.

In the analysis of the results of the pump−probe experiments presented in the next section it is shown that the product entrance channel interrogated by the probe radiation corresponds to electronically excited benzene. From our estimates of the dissociation quantum yield this is indeed the dominant entrance channel, but we are unable to establish whether this is the only channel of benzene formation. The benzaldehyde photodissociation product energy distribution certainly requires further investigation.

Dissociation Kinetics. The temporal evolution of the photodissociation of benzaldehyde following excitation to five single vibronic levels of the $S_2(\pi\pi^*) \leftarrow S_0$ band is summarized in Figure 3. The left-hand column shows the benzene and benzaldehyde ion currents as a function of the time delay between pump and probe lasers. The ion signal observed for m/e in the 102−108 amu range, represented by crosses in this figure, is attributed to benzaldehyde parent ions or to fragments of the type $C_6H_xCO^+$. The ion signal in the 74−80 amu range, represented by empty circles, is attributed to benzene or its fragment ions $C_6H_x^+$. While the benzaldehyde ion signal decays continuously with time, the benzene ion signal starts at zero, increases to a maximum at some intermediate time, and then decreases at long times. Note that at these five excitation wavelengths neither benzaldehyde nor benzene ions are detected when the probe laser is fired before the pump laser ($t < 0$).

The right-hand column of Figure 3 displays the same data plotted in semilogarithmic coordinates. This representation is particularly convenient as the two straight lines observed for the benzaldehyde ion yield reflect the biexponential decay of the excited states of benzaldehyde. The benzene ion signal, on the other hand, decays according to a single exponential with a rate that is independent of excitation energy. One aspect that is clearly perceived at high excitation energies is that benzene and benzaldehyde are observed to decay at approximately the same rate in the long time range. Since the time scale of this decay is approximately that expected for the translational motion of the molecular beam, we conclude that the decay of the benzaldehyde and the benzene ion currents observed in the long time range is due to the escape of excited molecules from the laser interaction region. A third curve displayed in this part of the figure corresponds to the logarithm of the sum of benzaldehyde and benzene ion yields. It illustrates an important aspect related to mass conservation to be discussed later. The increase in the dissociation rate with excitation energy is evident in both columns of Figure 3. The solid lines represent the results of a curve-fitting procedure following a kinetic model described in the next section.

Analysis and Discussion

The above results characterize the photodissociation of benzaldehyde as a predissociation process. Direct dissociation can be ruled out on the basis of the time dependence of the benzene ion signal observed in Figure 3 and the structured nature of the absorption and excitation spectra of benzaldehyde in this region. Figure 4 shows the energy level diagram for the photodissociation of benzaldehyde into benzene and carbon monoxide along with the ionization scheme and the kinetic model proposed for the reaction. For benzaldehyde, $T(n\pi^*)$, $S_1(n\pi^*)$, and $S_2(\pi\pi^*)$ lie 3.1, 3.3, and 4.4 eV above the vibrationless level of S_0,[1,29] respectively. The triplet $\pi\pi^*$ states have not been observed in the gas phase, but according to molecular orbital calculations,[1,37] the lowest excited triplet state is not the triplet $n\pi^*$ state observed in emission but a $\pi\pi^*$ state. According to our ab initio calculations,[1] there should be at least three triplet states below the origin of S_2 ordered as $T_1(\pi\pi^*)$, $T_2(n\pi^*)$, and $T_3(\pi\pi^*)$.

In the reaction $C_6H_5CHO \rightarrow C_6H_6 + CO$, two bonds are broken and two others are formed, resulting in a positive but small heat of reaction[38] ($\Delta H^\circ_{298} = 0.1$ eV mol^{-1}). Since the lowest excited triplet and singlet states of CO, $^3\Pi$ and $^1\Pi$, are located 6.0 and 8.1 eV above its $^1\Sigma^+$ ground electronic state,[39] the energy available to the reaction products, $E_{avl} = h\nu_{exc} - \Delta U^\circ_{298}$, is insufficient to produce electronically excited CO following excitation to S_2 in benzaldehyde. For this reason the electronic levels of CO are not included in the diagram. The ground state of benzene is positioned 0.1 eV above S_0 in benzaldehyde, based on the reaction energy. As its $T_1(^3B_{1u})$, $T_2(^3E_{1u})$, and $S_1(^1B_{2u})$ excited states are located 3.7, 4.5, and 4.7 eV above the ground state,[36,40,41] neither T_2 nor S_1 of benzene is accessible following excitation to the lowest levels of S_2 in benzaldehyde. Ionization potentials of benzaldehyde,[42] benzene,[43] and CO[44] are 9.51, 9.25, and 14.01 eV, respectively.

Two-color ionization results are analyzed on the basis of the premise that the F_2 laser radiation ionizes only electronically excited molecules. Ionization of benzaldehyde from the vibrationless level of S_0 requires the absorption of two photons of the 7.9 eV radiation, and such a process is much less probable than direct ionization and is not observed at the modest light intensities of the present experiment. Benzaldehyde molecules in vibrationally excited levels of S_0, if produced by internal conversion in the relaxation process, do not participate in the ionization scheme due to unfavorable Franck−Condon factors with the ionization continuum. Stepwise ionization of ground-state benzene molecules by the probe laser should not be appreciable since the 157 nm radiation of the F_2 laser falls between the $S_3(^1E_{1u})$ and the Rydberg absorption regions of benzene.[45] We have verified that irradiation of jet-cooled benzene with the probe laser produces negligible amounts of benzene ions. The ion signals displayed in Figure 3 therefore reflect the temporal evolution of the electronically excited states

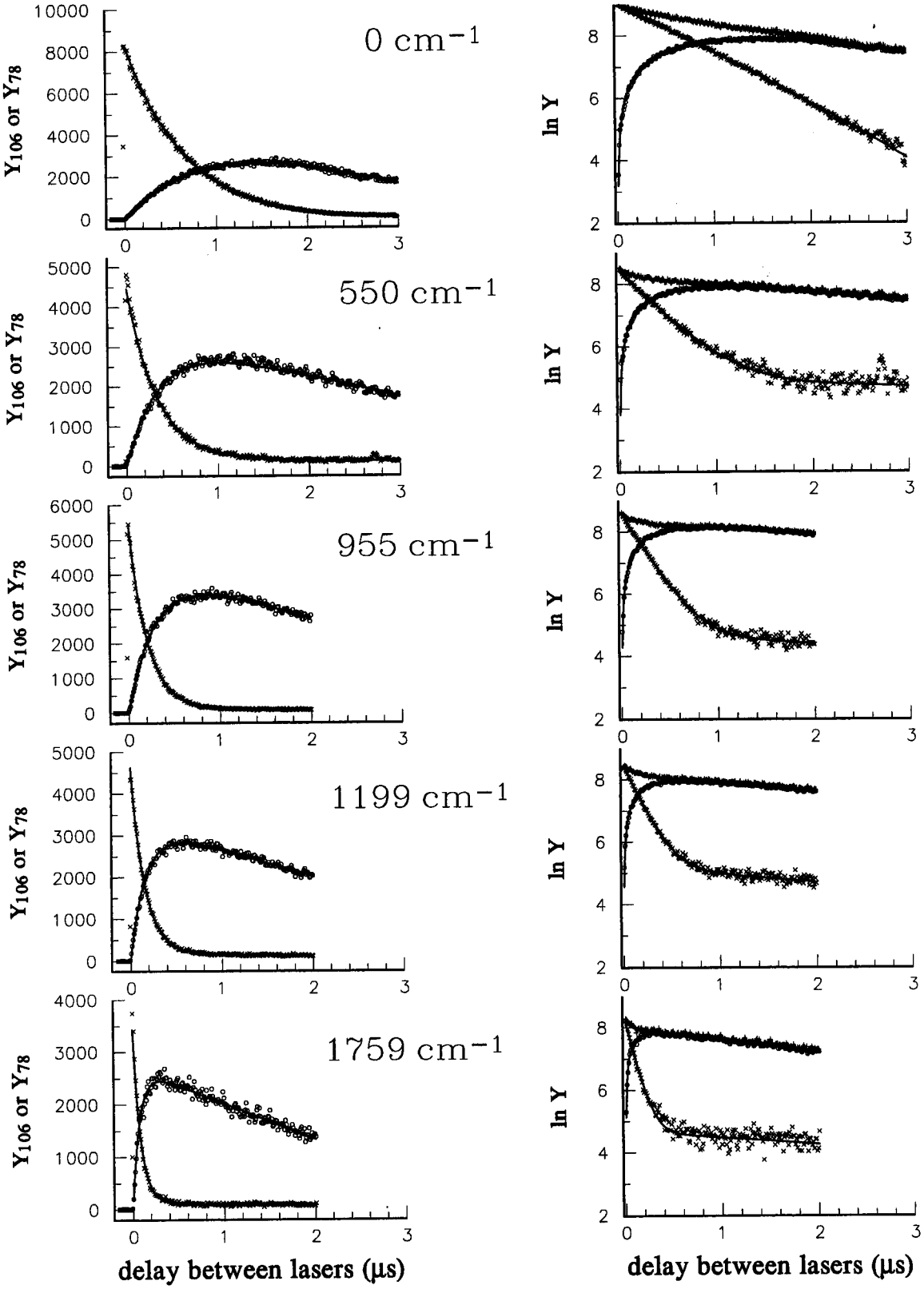

Figure 3. Effect of excess energy above the S_2 origin (35 191 cm^{-1}) on the dissociation rate of benzaldehyde into benzene and CO. Left column: benzaldehyde (×) and benzene (○) ion signals as a function of pump−probe delay time. Right column: logarithm of the benzaldehyde (×), benzene (○), and compounded benzaldehyde and benzene ion signals as a function of pump−probe delay time. The solid lines derive from the nonlinear least-squares fit described in the text.

of benzaldehyde and benzene. The excess energy available to benzaldehyde and benzene ions produced with this experimental arrangement is large enough to ensure that large Franck−Condon factors should be accessible[46−48] and that ionization efficiencies for all intermediate states involved in the two-color ionization scheme should be comparable.

The existence of two excited states that lead to ionization of benzaldehyde is inferred from the biexponential decay of the benzaldehyde ion signal. One of the states is short-lived ($\tau < 10^{-6}$ s), and its lifetime depends strongly on the energy of the pumped transition. The other state is long-lived ($\tau > 10^{-6}$ s), but its decay rate does not reflect its lifetime since it is strongly

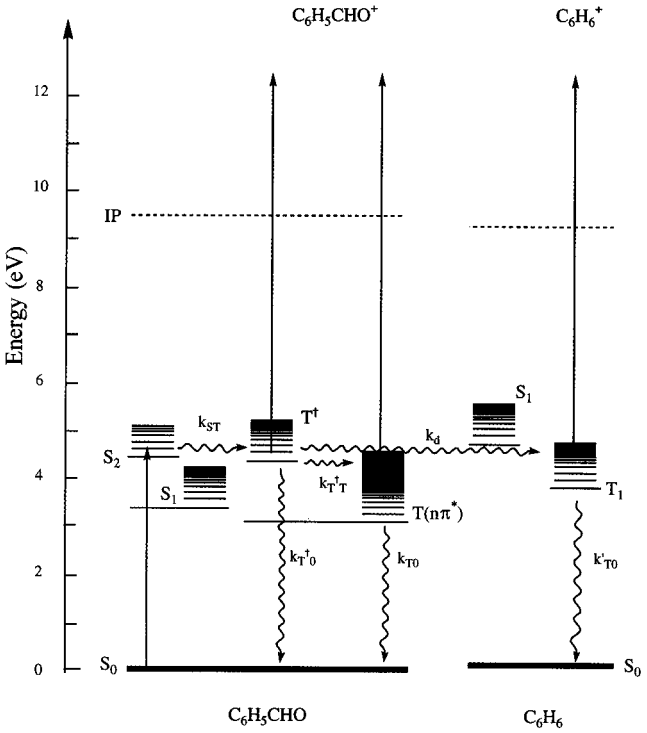

Figure 4. Energy level diagram for the photodissociation of benzaldehyde into benzene and CO showing the excited states involved, the pump−probe scheme, and the important relaxation pathways. $T^\dagger$ is a triplet state from which dissociation occurs. See text for rate constant definitions.

affected by sample translation. The benzene ion signal increases at short times when the benzaldehyde ion signal is rapidly decaying. Since the rate of benzene appearance and the rate of benzaldehyde disappearance in the short time range depend similarly on the vibronic level that is excited, the short-lived state of benzaldehyde is identified as the predissociating state. The decay of the benzene and benzaldehyde ion signals observed at long times is attributed to translation of reactant and product molecules out of the light interaction region. Since there are no signs of further buildup of the benzene ion signal in the long time range, we conclude that the long-lived state of benzaldehyde does not lead to benzene product formation.

The kinetic model depicted in Figure 4 is similar to those proposed by Baba and co-workers[5,6] and by Berger et al.[2] They interpreted the pressure-dependent behavior of the phosphorescence emission of benzaldehyde in terms of a competition between dissociation and collisional deactivation of a short-lived predissociating state with consequent population of a long-lived emitting state. As pointed out by them, the lifetimes of these states are both too long for singlet states. Based on radiative lifetime values determined from oscillator strength data and on fluorescence quantum yields measured to be less than 10^{-4}, the lifetimes of S_1 and S_2 of benzaldehyde have been estimated to be less than 4×10^{-10} and 10^{-12} s, respectively.[2,6,49] A preliminary inspection of Figure 3 indicates that the lifetime of the short-lived state of benzaldehyde that we observe, on the order of hundreds of nanoseconds, is much larger than either of these numbers. This short-lived predissociating state must therefore be a triplet state. From the evidence gathered so far, it could either be a vibrationally excited level of T(nπ*) or one of the T($\pi\pi$*) states of benzaldehyde. Because this could not be determined, the predissociating state is labeled $T^\dagger$ in Figure 4, and its origin has been arbitrarily positioned in this diagram. The long-lived state, on the other hand, is identified with T(nπ*) since the latter state is the origin of the weak phosphorescence emission that has been observed following excitation to S_2 under low-pressure conditions.[2,6] Under high-pressure conditions, the origin of T(nπ*) is the end point of the relaxation cascade in the electronically excited surface, as demonstrated by the strong emission observed from its vibrationless level.[2−8,22−24]

The relaxation paths and rate constants considered in the kinetic model are illustrated in Figure 4. The relaxation cascade starts with excited benzaldehyde molecules leaving the optically prepared S_2 state with rate constant k_{ST} and populating the short-lived predissociating state $T^\dagger$. Energy redistribution following the excitation step is expected to occur during the nanosecond laser pulse since k_{ST} is estimated to be greater than 10^{12} s^{-1} on the basis of the lifetime of the S_2 state mentioned above. Relaxation proceeds from $T^\dagger$ through multiple paths: dissociation into benzene and CO, identified by the rate constant k_d; internal conversion to T(nπ*), represented by the rate constant $k_{T^\dagger T}$; and relaxation to the ground electronic state, represented by the rate constant $k_{T^\dagger 0}$. The latter relaxation path, which includes radiative and nonradiative transitions to S_0, is formally considered for all states involved in the ionization scheme, although it should be slower than other relaxation processes under consideration. Assuming this rate constant to be on the same order as the equivalent relaxation rate in T(nπ*), $k_{T^\dagger 0}$ is expected to have a value in the 10^3-10^4 s^{-1} range.[31] The total decay rate for state $T^\dagger$ is given by $k_{T^\dagger} = k_d + k_{T^\dagger T} + k_{T^\dagger 0}$.

The long-lived T(nπ*) state is supposed to be populated by internal conversion from the predissociating state $T^\dagger$ and not by direct intersystem crossing from S_2 at the beginning of the relaxation cascade. (This supposition is based on the emission behavior of benzaldehyde under high pressures that suggests the emitting state is populated by the predissociating state.[2,6] This is also consistent with the rapid decay of the dissociating state of benzaldehyde evidenced in Figure 3.) Independent of which state feeds the long-lived state, the equations to be derived will have the same biexponential form. Decay routes considered for the long-lived state of benzaldehyde include radiative (phosphorescence) and nonradiative (ISC) transitions to the ground state with a combined rate constant k_{T0}. No reactive decay channels are expected for this state since the observed channel of benzene formation does not show any signs of a second entrance channel in the long time range.

Benzene molecules detected by two-color ionization in the present experiment are assumed to be formed in $T_1(^3B_{1u})$ since the probe radiation is not able to ionize ground-state benzene molecules and this is the only electronically excited state accessible in benzene following excitation to low levels of the S_2 state of benzaldehyde. Possible relaxation routes from this state include radiative and nonradiative transitions to S_0 represented by the rate constant k'_{T0}.

According to this kinetic model, the time dependence of the population of the excited states that lead to benzaldehyde and benzene ions is given by

short-lived state:

$$\frac{d[T^\dagger]}{dt} = -k_{T^\dagger}[T^\dagger] \qquad (1)$$

long-lived state:

$$\frac{d[T(n\pi^*)]}{dt} = k_{T^\dagger T}[T^\dagger] - k_{T0}[T(n\pi^*)] \qquad (2)$$

benzene:

$$\frac{d[^3B_{1u}]}{dt} = k_d[T^\dagger] - k'_{T0}[^3B_{1u}] \quad (3)$$

Solution of the coupled differential equations gives the following expressions for the benzaldehyde (N_{106}) and the benzene (N_{78}) excited-state populations:

$$N_{106} \propto [T^\dagger] + [T(n\pi^*)] = A_I e^{-k_{T^\dagger}t} + A_{II} e^{-k_{T0}t} \approx A_I e^{-k_{T^\dagger}t} + A_{II} \quad (4)$$

$$N_{78} \propto [^3B_{1u}] = B(e^{-k'_{T0}t} - e^{-k_{T^\dagger}t}) \approx B(1 - e^{-k_{T^\dagger}t}) \quad (5)$$

where A_I, A_{II}, and B are coefficients that depend on the population of excited molecules at time $t = 0$ and on the individual rate constants k_d, $k_{T^\dagger T}$, $k_{T^\dagger 0}$, k_{T0}, and k'_{T0}. Note that, since k_{ST} is fast compared to the laser pulse duration, the population of $T^\dagger$ at the end of the pump laser pulse is expected to be equal to the total population of excited molecules at time $t = 0$. The population of all other states at this time is assumed to be zero. The approximations indicated in eqs 4 and 5 are valid if k_{T0} and k'_{T0} are at least 2 orders of magnitude smaller than $k_{T^\dagger}$. Furthermore, with the latter rate constant being in the 10^6-10^7 s^{-1} range and the rate of escape of excited molecules out of the light interaction region being on the order of 10^5 s^{-1}, any photophysical relaxation process occurring at a rate slower than 10^5 s^{-1} would be masked by this sample translation effect. According to the data presented in Figure 3, the latter effect is indeed dominant since the benzaldehyde and the benzene ion signals in the long time range appear to decay at the same rate independent of excitation energy.

To establish the relation between the excited-state populations (N_{106} and N_{78}) and the observed ion yields (Y_{106} and Y_{78}), we multiplied the approximate forms of eqs 4 and 5 by two factors. To account for possibly different absorption cross sections of the excited species that participate in the ionization scheme, the populations of $T^\dagger$, $T(n\pi^*)$, and $^3B_{1u}$ are multiplied by a factor corresponding to the ionization efficiency of each specific state: $\eta_{T^\dagger}$, η_T, and η_{78}, respectively. The other factor is a detection probability function $P(t)$ that is used to account for sample translation. It represents the probability of finding an excited molecule in the laser interaction volume at a given time after the excitation step. The expressions thus obtained for the observed ion yields are

$$Y_{106} = P(t)(\eta_{T^\dagger}A_I e^{-k_{T^\dagger}t} + \eta_T A_{II}) \quad (6)$$

$$Y_{78} = P(t)\eta_{78}B(1 - e^{-k_{T^\dagger}t}) \quad (7)$$

In treating the effect of sample translation, we examined a few different forms of the detection probability function. A time-delayed cross-correlation of the pump volume with the probe volume should result in an adequate description of this function, but it does require information concerning laser beam shapes. Due to the uncertainty concerning the spatial profiles of the light reported in the Experimental Section, cross-correlation functions were calculated considering two possible types of beam shapes, rectangular and Gaussian. Each type of cross-correlation function was calculated over a range of possible values. One function that proved to be very useful in the data analysis was that resulting from two light beams with rectangular profiles of equal sizes. In this case the detection probability function is a simple analytic expression that depends on a single parameter: $P(t) = 1 - at$. Another simple function used in the data analysis treated translation as a first-order process with an effective rate constant of k_{tr}. The resulting detection probability function decays exponentially with time according to $P(t) = e^{-k_{tr}t}$. This model preserved the functional forms of eqs 4 and 5 that predict the observed double-exponential decay of the benzaldehyde signal and the single-exponential decay of the benzene signal.

The experimental benzaldehyde and benzene ion signals were fitted to eqs 6 and 7, respectively, using a nonlinear least-squares routine based on a modified Marquardt algorithm.[50] From the exponential factors in both equations the decay rate of the short-lived state of benzaldehyde and the benzene product growth rate were independently determined along with the preexponential factors. The set of parameters representing beam sizes that resulted in the best fit were also assessed.

All models tested were able to provide good fits as long as laser beam parameters were allowed to vary from experiment to experiment. They all yielded rather similar values for the decay rate of the short-lived state of benzaldehyde but not for the benzene growth rate. While benzaldehyde parameters were determined with an uncertainty of less than 20%, benzene parameters turned out to be very sensitive to the shape of the function $P(t)$, and the resulting values were subject to an uncertainty on the order of 30−50%. This is understood in terms of the functional forms of eqs 6 and 7 as the benzene ion signal is given by a difference of two terms, one representing product appearance and the other product disappearance. Changes in one term affect the value of the other term more drastically than in the case of the benzaldehyde ion signal, in which two terms representing disappearance rates are added together. This effect is worse at low excitation energies since appearance and disappearance rates differ only by 1 order of magnitude under these conditions.

The escape rate due to sample translation was determined to be in the $2.5-5.0 \times 10^5$ s^{-1} range using the k_{tr} parameter and in the $1.5-3.0 \times 10^5$ s^{-1} range with the a parameter. The spread in the values of these parameters appeared to be due to laser beam variations in different experiments since no wavelength dependence was observed. The cross section of the probe laser beam was not necessarily the same from run to run since the apertures disposed along the beam path were moved in order to maximize the overlap between the two light beams and, at the same time, minimize the light scattered onto the walls of the instrument. At higher excitation energies, however, all models performed equally well and the escape parameters displayed a smaller spread. This is because small variations in beam size do not affect the shape of the detection probability curve in the short time range as much as they do at longer times.

Table 1 lists the decay rate of the short-lived predissociating state of benzaldehyde ($k_{T^\dagger}$) and the growth rate of the benzene product ($k'_{T^\dagger}$) as a function of excess energy within the S_2 band. Values listed correspond to the average of the rate constants obtained from the best fits at each excitation wavelength. As seen in Figure 3, agreement between model and experiment is indeed very good. The fitted curves displayed in that figure are those obtained with the linear form of the detection probability function. The measured decay rate of the predissociating state shown in Table 1 is strongly dependent on excitation frequency, and its value increases by an order of magnitude within the investigated range ($\sim$1800 cm^{-1}). Figure 5 shows the dependence of this rate constant on excitation energy. The increase is exponential, as indicated by the dotted curve, and there are no indications of mode specific effects. This behavior is consistent with that of a statistical reaction, as

TABLE 1: Rate Constants and Quantum Yields for the Dissociation of Benzaldehyde as a Function of Excess Energy in S_2

excess energy (cm^{-1})	$k_{T^\dagger} \times 10^{-6a}$ (s^{-1})	$k'_{T^\dagger} \times 10^{-6b}$ (s^{-1})	$\phi^{B}_{dis}{}^{c}$	$\phi^{A}_{dis}{}^{d}$
0	1.2	1.1	0.72	1.00
400	2.5	1.6	0.71	0.99
550	3.0	2.8	0.69	0.96
800	4.0	3.0	0.60	0.98
955	4.9	3.5	0.76	0.98
1200	6.4	6.0	0.68	0.96
1359	7.8	7.8	0.80	0.98
1502	10.3	9.5	0.79	0.95
1759	12.0	12.5	0.72	0.97

[a] Decay rate of the short-lived state of benzaldehyde. [b] Benzene appearance rate. [c] Dissociation quantum yield defined in terms of benzene's ion signal: $\phi^{B}_{dis} = (\eta_{106}/\eta_{78}) \times B^{Y}/(A^{Y}_{I} + A^{Y}_{II})$. [d] Dissociation quantum yield defined in terms of benzaldehyde's ion signal: $\phi^{A}_{dis} = A^{Y}_{I}/(A^{Y}_{I} + A^{Y}_{II})$.

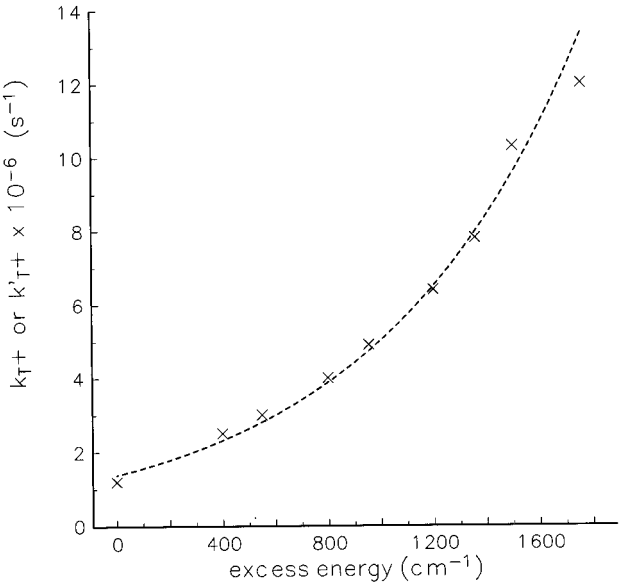

Figure 5. Dependence of the rate constant for the loss of benzaldehyde, $k_{T^\dagger}$, on vibrational energy in S_2. The dotted line corresponds to an exponential fit of the decay rate $k_{T^\dagger}$.

complete randomization of the deposited energy takes place prior to the dissociation step.

According to the kinetic model presented the benzene product is expected to appear at the same rate as the predissociating state $T^\dagger$ decays. As seen in Table 1, six of the nine pairs of rate constants are in good agreement. Due to the uncertainties related to the benzene data fit mentioned above, it is unlikely that differences between reactant disappearance and product appearance rates shown in Table 1 represent anything more than experimental error. To derive more accurate values for the product appearance rate, the effect of molecular translation should be eliminated. An experimental setup in which the pump beam propagates coaxially with the molecular beam not only should lead to more precise values of the benzene growth rate but also should confirm the assumptions made here concerning the slow photophysical relaxation rates of product and reactant.

Our results are found to be in rough agreement with those of Polevoy et al.[17] Their reported value for the rate constant $k_{T^\dagger}$ at the S_2 origin, 1.6×10^6 s^{-1}, is similar to the 1.5×10^6 s^{-1} value that we find when signal decay due to sample translation is incorporated in the rate constant $k_{T^\dagger}$. Our results, however, show a monotonic increase of the rate constant $k_{T^\dagger}$ with excess energy, while theirs show strong fluctuations. This is understood in terms of the effect of different thermal vibrational energy distributions on the measured energy-dependent rate constants $k_{T^\dagger}(E)$. Under the jet-cooled conditions of our experiment, the energy distribution of the excited molecules is much narrower than it would be for a room-temperature sample so that incoherent averaging caused by simultaneous dissociation of several dissociation channels is minimized. Yet another difference concerning our results and theirs is related to the behavior of the benzene signal in the long time range as a function of excitation energy. They reported an increase in the benzene decay rate with excess energy and suggested it might be due to changes in the relaxation rate k'_{T0}. However, as long as this rate constant is significantly smaller than 10^5 s^{-1}, any changes in its value with excitation energy are not detected with our experimental arrangement. It seems unlikely that it would be observable with their apparatus.

The benzaldehyde decay rate at the S_2 origin reported here can also be compared with those determined from quenching measurements at 284 nm: 3.2×10^5 s^{-1} [6] and 1.14×10^6 s^{-1}.[8] The latter agrees well with our value of $(1.2 \pm 0.2) \times 10^6$ s^{-1}.

The dissociation quantum yield was estimated using the preexponential factors of eqs 6 and 7. According to the kinetic model presented, the efficiency of formation of triplet benzene can be written as $k_d/k_{T^\dagger}$ in terms of the rate constants or as $B/(A_I + A_{II})$ in terms of the population coefficients. If we consider that there is only one reaction channel open, the one leading to $^3B_{1u}$ benzene, then the efficiency of formation of triplet benzene corresponds to the dissociation quantum yield, ϕ_{dis}. Furthermore, if dissociation into this channel and internal conversion to T(nπ*) are the main relaxation routes for molecules in $T^\dagger$, i.e. $k_{T^\dagger} \approx k_d + k_{T^\dagger T}$ as previously assumed, then the dissociation quantum yield can also be expressed as $A_I/(A_I + A_{II})$. The parameters experimentally assessed, the preexponential factors of eqs 6 and 7, A^{Y}_{I}, A^{Y}_{II}, and B^{Y}, are related to the population coefficients above by $A^{Y}_{I} = A_I\eta_{T^\dagger}$, $A^{Y}_{II} = A_{II}\eta_T$ and $B^{Y} = B\eta_{78}$. Although ionization efficiencies have not been determined, it seems reasonable to expect that $T^\dagger$ and T(nπ*) benzaldehyde molecules will have similar ionization cross sections at 157 nm: the two states have the same multiplicity, they may even have the same overall symmetry, and their origins are not far apart. By assuming a single value for the ionization efficiency of both states of benzaldehyde and naming it η_{106}, the two expressions for the dissociation quantum yields derived above can be written as $\phi^{B}_{dis} = (\eta_{106}/\eta_{78})B^{Y}/(A^{Y}_{I} + A^{Y}_{II})$ and $\phi^{A}_{dis} = A^{Y}_{I}/(A^{Y}_{I} + A^{Y}_{II})$.

The last two columns of Table 1 list our best estimates of the dissociation quantum yield as a function of excess energy according to the latter expressions. The values are subject to uncertainties on the order of 40−70% for ϕ^{B}_{dis} and 20−30% for ϕ^{A}_{dis}. The fluctuations observed in the values of ϕ^{B}_{dis} are understood in terms of the large uncertainties involved in the benzene data fit. Although uncertainties are large enough to hide any wavelength dependence that might occur, two points are noteworthy. First, ϕ^{A}_{dis} is found to be greater than 0.9 at all excitation energies. That indicates that deactivation of $T^\dagger$ through internal conversion to T(nπ*) occurs with an efficiency of less than 0.1 if ionization cross sections of $T^\dagger$ and T(nπ*) benzaldehyde are taken to be equal. Second, there is a systematic difference between the values of the dissociation quantum yield estimated using the benzene population coefficient ($\phi^{B}_{dis} = 0.6-0.8$) and that estimated using only benzaldehyde coefficients ($\phi^{A}_{dis} > 0.9$) at each excitation energy. While this difference may be due to the large uncertainties involved in deriving ϕ^{B}_{dis}, we note that this result is consistent with the observed behavior of the total ion yield: as displayed in the right-hand column of Figure 3, the sum of the benzene

and benzaldehyde signals drops at a faster rate in the time range that benzaldehyde dissociates. Altogether, these observations indicate either that the ionization efficiency of benzene is indeed different from that of benzaldehyde or that there are other routes of relaxation available for molecules in $T^{\dagger}$ that lead to nonionizable species. The wavelength dependence of the benzene ion signal shown in Figure 2 suggests that at least some benzene molecules are formed in the ground electronic state when benzaldehyde is irradiated at 258.9 nm, and it is reasonable to expect this product entrance channel to be open at other excitation wavelengths as well. Although we cannot be sure if part of the signal recorded in this case is not due to a benzene impurity in the benzaldehyde sample, this observation indicates the need for further experiments capable of probing the population of ground-state benzene molecules following excitation of benzaldehyde in order to establish the benzene state distribution as a function of excitation wavelength. Together with the determination of excited-state ionization efficiencies such measurements should provide further insight concerning the product distribution in the photodissociation of benzaldehyde.

Conclusions

A pump−probe mass spectrometry technique has been used to investigate the photodissociation of benzaldehyde into benzene and CO following excitation to the S_2 state, revealing a number of aspects concerning the kinetics and dynamics of this dissociation process. From the observed biexponential decay of the benzaldehyde signal it has been inferred that two metastable states are populated in the relaxation process. The time dependence of the reactant and benzene product signal indicates that dissociation occurs from the short-lived state of benzaldehyde on a time scale of hundreds of nanoseconds. The dissociation rate increases with vibrational energy, and there is no suggestion of mode selective behavior. According to the analysis presented, benzene molecules are produced in its lowest triplet state. The threshold for dissociation along this channel is located somewhere below the origin of the S_2 state of benzaldehyde since it is possible to detect benzene molecules following excitation to the S_2 vibrationless level. The efficiency of formation of triplet benzene molecules as a function of excitation energy has been estimated, but the values obtained depend on the unknown ionization efficiencies of the excited species involved in the ionization scheme. The existence of a secondary entrance channel leading to benzene molecules in the ground electronic state has been suggested since enhancement of the benzene signal at excitation frequencies corresponding to allowed transitions of the $S_1 \leftarrow S_0$ spectrum of benzene has been observed, but this product entrance channel needs to be further investigated and characterized.

Acknowledgment. C.R.S. thanks Brazilian CNPq for financial support and Universidade Federal do Rio de Janeiro for a leave of absence. This work has been supported by the U.S. National Science Foundation.

Registry No. Benzaldehyde, 100-52-7.

References and Notes

(1) Silva, C. R.; Reilly, J. P. *J. Phys. Chem.* **1996**, *100*, 17111.
(2) Berger, M.; Goldblatt, I. L.; Steel, C. *J. Am. Chem. Soc.* **1973**, *95*, 1717.
(3) Bruhlmann, U.; Nonella, M.; Russegger, P.; Huber, J. R. *Chem. Phys.* **1983**, *81*, 439.
(4) Metcalfe, J.; Brown, R. G.; Phillips, D. *J. Chem. Soc., Faraday Trans. 2* **1975**, *71*, 409.
(5) Itoh, T.; Takemura, T.; Baba, H. *Chem. Phys. Lett.* **1976**, *40*, 481.
(6) Itoh, T.; Baba, H.; Takemura, T. *Bull. Chem. Soc. Jpn.* **1978**, *51*, 2841.
(7) Bruhlmann, U.; Huber, J. R. *Chem. Phys. Lett.* **1979**, *66*, 353.
(8) Hirata, Y.; Lim, E. C. *J. Chem. Phys.* **1980**, *72*, 5505.
(9) Antonov, V. S.; Knyazev, I. N.; Letokhov, V. S.; Matyuk, V. M.; Movshev, V. G.; Potapov; V. K. *Opt. Lett.* **1978**, *3*, 37.
(10) Antonov, V. S.; Letokhov, V. S.; Shibanov, A. N. *Appl. Phys.* **1980**, *22*, 293.
(11) Antonov, V. S.; Letokhov, V. S. *Appl. Phys.* **1981**, *24*, 89.
(12) Antonov, V. S. *Opt. Spectrosc. (USSR)* **1982**, *52*, 5.
(13) Long, S. R.; Meek, J. T.; Harrington, P. J.; Reilly, J. P. *J. Chem. Phys.* **1983**, *78*, 3341.
(14) Yang, J. J.; Gobeli, D. A.; Pandolfl, R. S.; El-Sayed, M. A. *J. Phys. Chem.* **1983**, *87*, 2255.
(15) Yang, J. J.; Gobeli, D. A.; El-Sayed, M. A. *J. Phys. Chem.* **1985**, *89*, 3426.
(16) Polevoy, A. V.; Matyuk, V. M.; Grigor′eva, G. A.; Potapov, V. K. *Khim. Vys. Energ.* **1984,** *18*, 195.
(17) Polevoy, A. V.; Matyuk, V. M.; Potapov, V. K. *Sov. J. Chem. Phys. (Engl. Transl.)* **1990**, *6*, 1157; *Khim. Fiz.* **1987**, *6*, 620.
(18) Prileshajewa, N. *Acta Physichochim. URSS* **1935**, *3*, 195.
(19) Schüler, H.; Reinebeck, L. *Z. Naturforsch.* **1950**, *5A*, 448.
(20) Asundi, R. K.; Battacharya, B.; Appalanarasimham, N. *Curr. Sci. (India)* **1952**, *21*, 273.
(21) Robinson, G. W. *J. Chem. Phys.* **1954**, *22*, 1384.
(22) Stockburger, M. *Z. Phys. Chem. (Frankfurt)* **1962**, *31*, 350.
(23) Hollas, J. M.; Thakur, S. N. *Chem. Phys.* **1973**, *1*, 385.
(24) Koyanagi, M.; Goodman L. *Chem. Phys.* **1979**, *39*, 237.
(25) Almasy, F. *J. Chim. Phys.* **1933**, *30*, 528, 634.
(26) Garg, S. N. *J. Sci. Res. Banaras Hindu Univ.* **1951**−**52**, *2*, 153.
(27) Imanishi, S.; Semba, K.; Ito, M.; Anno, T. *Bull. Chem. Soc. Jpn.* **1952**, *25*, 150.
(28) Abe, H.; Kamei, S.; Mikami, N.; Ito, M. *Chem. Phys. Lett.* **1984**, *109*, 217.
(29) Ohmori, N.; Suzuki, T.; Ito, M. *J. Phys. Chem.* **1988**, *92*, 1086.
(30) Villa, E.; Amirav, A.; Chen, W.; Lim, E. C. *Chem. Phys. Lett.* **1988**, *147*, 43.
(31) Sneh, O.; Cheshnovsky, O. *J. Phys. Chem.* **1991**, *95*, 7154.
(32) Colby, S. M.; Reilly, J. P. *Int. J. Mass Spectrom. Ion Processes* **1994**, *131*, 125.
(33) Walsh, A. D. *Trans. Faraday Soc.* **1946**, *42*, 62.
(34) Kimura, K.; Nagakura, S. *Theor. Chim. Acta* **1965**, *3*, 164.
(35) Atkinson, G. H.; Parmenter, C. S. *J. Mol. Spectrosc.* **1978**, *73*, 20.
(36) Stephenson, T. A.; Radloff, P. L.; Rice, S. A. *J. Chem. Phys.* **1984**, *81*, 1060.
(37) Inuzuka, K.; Yokota, T. *Bull. Chem. Soc. Jpn.* **1965**, *38*, 1055.
(38) Pedley, J. B.; Naylor, R. D.; Kirby, S. P. *Thermochemical Data of Organic Compounds*; Chapman and Hall: New York, 1986.
(39) Herzberg, G. *Molecular Spectra & Molecular Structure Vol. I: Spectra of Diatomic Molecules*; Kriger: Malabar, 1989.
(40) Parmenter, C. S. *Adv. Chem. Phys.* **1972**, *22*, 365.
(41) Sharpe, S.; Johnson, P. *J. Chem. Phys.* **1984**, *81*, 4176.
(42) Rosenstock, H. M.; Draxl, K.; Steiner, B. W.; Herron, J. T. *J. Phys. Chem. Ref. Data* **1977**, *6*, Suppl. 1.
(43) Grubb, S. G.; Whetten, R. L.; Albrecht, A. C.; Grant, E. R. *Chem. Phys. Lett.* **1984**, *108*, 420.
(44) *Handbook of Chemistry and Physics*; Lide, D. R., Ed.; CRC: New York, 1996.
(45) Hiraya, A.; Shobatake, K. *J. Chem. Phys.* **1991**, *94*, 7700.
(46) Dietz, T. G.; Duncan, M. A.; Smalley, R. E. *J. Chem. Phys.* **1982**, *76*, 1227.
(47) Johnson, P. M.; Otis, C. E. *Annu. Rev. Phys. Chem.* **1981**, *32*, 139.
(48) Otis, C. E.; Knee, J. L.; Johnson, P. M. *J. Phys. Chem.* **1983**, *87*, 2232.
(49) Kanda, Y.; Kaseda, H.; Matumura, T. *Spectrochim. Acta* **1964**, *20*, 1387.
(50) *Numerical Recipes in Pascal: The Art of Scientific Computing*; Cambridge University: Cambridge, 1989.